

Sturm-Liouville Equation: The Bridge between Eigenvalue and Green's Function Problems

L. SEVGİ

*Electronics and Communication Engineering Department, Doğuş University,
Zeamet Sok. No 22, Kadıköy, İstanbul-TURKEY
lsevgi@dogus.edu.tr*

Abstract

This article is intended as an educational aid and discusses guided wave propagation problems that are modeled via the Sturm-Liouville equation in electromagnetics. The bridge between source-free (eigenvalue) and source-driven (Green's function) problems that are represented by the same Sturm-Liouville equation is emphasized. The presentation focuses on representation of an arbitrary source from the features (eigenfunctions) of the problem geometry and extraction of the eigenvalues of a problem from propagation characteristics (Green's function) on a canonical problem; a homogeneously filled parallel plate waveguide with non-penetrable boundaries.

1. Introduction

The strategy in solving Maxwell's equations under given boundary/initial conditions and sources is problem-dependent. It is quite different for an antenna radiation in open space than for a radiating element inside a waveguide, or a radar cross section (RCS) problem. In most electromagnetic (EM) engineering problems, there are 2 approaches [1]:

- Reduce and solve the problem in terms of transverse and longitudinal components for most of the waveguiding environments. Here, the problem not only is reduced, but is also solved.
- Simplify the full wave equations at the beginning by using vector and scalar potentials. The scalarization of these auxiliary functions is the second step. In this case, one needs to use equations that relate vector/scalar potentials to the electric and magnetic fields.

For example, propagation through rectangular waveguides, resonators, and microstrip networks are better handled via approach 1. On the other hand, approach 2 is used in most antenna radiation and RCS problems.

The analysis and synthesis of source-driven EM propagation problems is effectively accomplished in the complex configuration (space-time) – spectrum (wavenumber-frequency) phase space and it decomposes space-time-dependent wave functions into their spectral constituents. Having $\vec{r} = (x, y, z)$ and $\vec{k} = (k_x, k_y, k_z)$ as the spatial and wavenumber vectors, respectively, the configuration space function $G(\vec{r}, t)$

(i.e., transient point source response, which is called Green's function) can be represented via phase space components $\bar{G}(\vec{r}, t, \vec{k}, \omega)$ as [1]

$$G(\vec{r}, t) = \int \iiint \bar{G}(\vec{r}, t, \vec{k}, \omega) d\vec{k}d\omega \tag{1}$$

The configuration (space-time) – spectrum (wavenumber-frequency) phase space of a problem can be accessed via continuous and discrete local and global transforms that are derived from Eq. (1). Coordinate separable canonical geometries provide great flexibility and opportunity for visual illustrations to the analytical modeler. For example, the 2D non-penetrable (perfectly electrical conductor (PEC)) parallel plate waveguide is an excellent structure for these illustrations; therefore, it is used in this article in numerical demonstrations.

A generic problem for a source-driven structure is the Green's function (GF) problem. The GF is the response of a linear system to a point source of unit strength. A source of unit strength at a position “a” along, for example, z coordinate can be represented by the Dirac Delta function $\delta(z - a)$. The general form of a GF problem may be postulated via a second-order non-homogeneous differential equation with a delta function on the right-hand side, together with boundary conditions (BCs) that represents the geometry of the problem. Omitting the delta function on the right-hand side (i.e., using a homogeneous second-order differential equation and BCs) yields the source-free (i.e., an eigenvalue) problem. An eigenvalue problem is to find a set of complete functions that characterize the geometry of the problem (and yields eigenmodes and eigen spectral wavenumbers that describe source-free wave fields, which individually satisfy BCs in wave-confining environments). Many EM problems, either source-free or source-driven, can be represented by a unique second-order differential equation; the Sturm-Liouville (SL) equation (see Eq. (2a) below). Solving the SL equation when λ is a fixed parameter yields nothing but the GF. GF solution may also be built from eigenfunction solutions. Alternatively, eigenfunctions may also be derived from the GF solution. It illustrates that a guided wave problem may be handled as either an eigenvalue problem or a GF problem, since the former yields the latter and vice versa (see Figure 1).

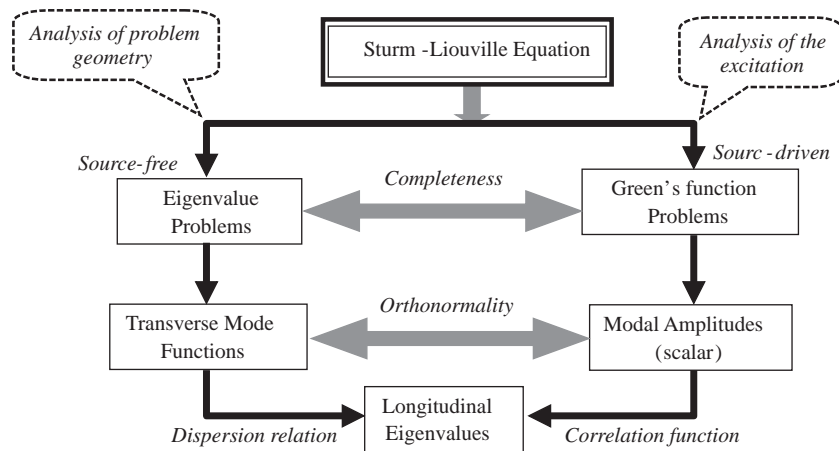


Figure 1. SL equation and representation of source-free (eigenvalue) and source-driven (GF) problems.

2. Sturm-Liouville (SL) Equation

Many of the boundary value problems in EM lead to the Sturm-Liouville (SL) equation. The SL equation is of the form

$$\left[\frac{d}{dz} p(z) \frac{d}{dz} - q(z) + \lambda w(z) \right] g(z, z'; \lambda) = -\delta(z - z') \quad (2a)$$

and the BCs at z_1 and z_2 ($z_1 < (z, z') < z_2$). Here, p , q , and w are, in general, real, and continuous functions of z that correspond to geometrical quantities of the problem, and λ is a spectral parameter (not the wavelength). The three common BCs are

$$\begin{aligned} g &= 0 \text{ at } z = z_1 \text{ and } z_2 \text{ (Dirichlet, DBC)} \\ dg/dz &= 0 \text{ at } z = z_1 \text{ and } z_2 \text{ (Neumann),} \\ g + \alpha dg/dz &= 0 \text{ at } z = z_1 \text{ and } z_2 \text{ (Cauchy, CBS)} \end{aligned} \quad (2b)$$

where α is a parameter. There are 3 types of SL problems [2]. SL1 corresponds to the finite interval and real λ (i.e., p , q , and w are real and continuous functions of z , z_1 , and z_2 are finite, and λ is real and independent of z) case, while SL2 belongs to the complex λ (i.e., p , q , and w are real and continuous functions of z , z_1 , and z_2 are finite, and λ is real and independent of z). Finally, if any of these conditions is violated (e.g., p , q , or w is not a continuous function of z , either or both of z_1 and z_2 are infinite, etc.) it is an SL3 problem.

The SL equation in Eq. (2a) models [3]:

- Transmission line system directly if λ is a given fixed parameter (GF problem).
- An eigenvalue problem (when the equation is homogeneous, i.e., right-hand side is zero) where λ is a free parameter (that CAN NOT be an eigenvalue). So, the condition for uniqueness for this case can easily be satisfied when λ is assumed complex, i.e., $\text{Im} \{ \lambda \} \neq 0$ (since eigenvalues are real when p , q , and w are real).

Various canonical problems that are represented by SL equations for different sets of parameters are listed in Table 1. 1D wave and the Airy equation in Cartesian coordinates, the Bessel equation in cylindrical, and Legendre polynomials in spherical coordinates are only a few examples. It is well-known that the Airy equation is met in many wave propagation problems above a surface with vertical linear refractivity profiles (e.g., surface and/or elevated ducting conditions in ground wave propagation problems). Similarly, the Bessel equation is the characteristic radial wave equation in cylindrical coordinates for structures; for example, cylindrical waveguides, optical fibers, radial and co-axial transmission lines, wedge geometries, etc.

Table 1. Reduced SL equations under different parameter sets

SL Equation		system	Solution
$\left[\frac{d^2}{dz^2} - k_z^2 \right] U_z(z) = f(z)$	$p = 1, q = 0$ $w = 1, \lambda = k_z^2$	Cartesian	Oscillatory (sine or cosine functions) for finite region, progressing (exponential functions) for infinite region
$\left[\frac{d}{dz} z \frac{d}{dz} - v^2 + k_z^2 z^2 \right] U_z(z) = f(z)$	$p = z, q = v^2$ $w = z^2, \lambda = k_z^2$	Cylindrical	Bessel functions ($J_\nu(z), N_\nu(z), H_\nu^{1,2}(z)$)
$\left[\frac{d^2}{dz^2} - k_z^2 z \right] U_z(z) = f(z)$	$p = 1, q = 0$ $w = z, \lambda = k_z^2$	Cartesian	Airy functions ($AI(z), Bi(z), W_{1,2}(z)$)
$\left[-\frac{d}{dz}(1-z^2) \frac{d}{dz} - n(n-1) \right] U_z(z) = f(z)$	$p = 1 - z^2, q = 0$ $w = 1,$ $\lambda = n(n-1)$	Spherical	Legendre polynomials ($P_n^m()$)

2.1. Source-free solutions: The eigenvalue problem

Once the BCs are specified for a given problem, the homogeneous SL equation in the form of

$$\left[\frac{d}{dz} p(z) \frac{d}{dz} - q(z) + \lambda w(z) \right] U(z) = 0 \tag{3}$$

yields an infinite set of solutions $U(z) = U_n(z)$ that correspond to particular values of $\lambda = \lambda_n$. The functions $U_n(z)$ are called eigenfunctions and the values λ_n are eigenvalues. In all cases, $U_n(z)$ forms an orthogonal set of functions over the finite interval of $z_1 < z < z_2$ and orthogonality is given as

$$\int_{z_1}^{z_2} w(z) U_n(z) U_m(z) = 0 \tag{4}$$

i.e., $U_n(z)$ forms an orthogonal set with respect to the weighing function $w(z)$. Each of the functions in the orthogonal set (preferably) has unit energy, so they are also normalized. The orthonormality condition is then given as

$$\int_{z_1}^{z_2} w(z) U_n(z) U_m(z) = \begin{cases} 1 & n = m \\ 0 & n \neq m \end{cases} \tag{5}$$

Superposition of source-free solutions (eigenfunctions) must form a complete set. A set of functions defined over some interval, and subject to stated BC at its ends is said to be complete if any function in

this interval can be expressed as a linear combination of them. Since the most peculiar function is the delta function, a complete set of functions is the set that can be represented in terms of delta functions:

$$\frac{\delta(z - z')}{w(z')} = \sum_n U_n(z) U_n^*(z') \quad (6)$$

where (*) denotes the complex conjugate.

2.2. Source-driven solutions: The Green's function (GF) problem

The GF $g(z, z', \lambda)$ is the response of a linear system (i.e., solution of the SL equation) to a point source of unit strength. A source of unit strength at the position $z = z'$ can be represented by the Dirac delta function as given on the right hand side of Eq. (2a). The GF satisfies a homogeneous SL equation (3) at all points, except $z \neq z'$. At $z = z'$, GF must be continuous, but its first derivative is discontinuous by a unit amount, so that the second derivative then yields a delta function singularity.

The GF of a problem can be constructed via 2 different ways [1-3]; an eigenfunction expansion may be used,

$$g(z, z'; \lambda) = \sum_{n=1}^{\infty} \frac{U_n(z) U_n^*(z')}{\lambda - \lambda_n} \quad (\text{Method I}) \quad (7)$$

or 2 solutions that satisfy Eq. (1) together with the right and left hand BCs, respectively, may be matched at the source location via Eq. (1), that is

$$g(z, z', \lambda) = -\frac{f_1(z_<)f_2(z_>)}{p(z')W(z')} \quad (\text{Method II}) \quad (8)$$

where $z_<$ is the lesser of z or z' , and $z_>$ is the greater of z or z' . Here, $f_1(z_<)$ and $f_2(z_>)$ are the solutions of Eq. (3) and satisfy the BCs at the left-end (z_1) and right-end (z_2), respectively, and $W(z')$ is called the Wronskian, which is a global constant and can be calculated from

$$W = \left(f_1(z) \frac{df_2(z)}{dz} - f_2(z) \frac{df_1(z)}{dz} \right) \quad \text{at any point between } z_1 - z_2 \quad (9)$$

Constructing the GF is adequate to solve an SL equation for any kind of excitation under specified BCs, since the excitation can be represented as a superposition of point sources. The delta function is symmetric, i.e., $\delta(z - z') = \delta(z' - z)$, whence $g(z, z', \lambda) = g(z', z, \lambda)$, thereby exhibiting reciprocity under the interchange of source and observation points. Finally, any field distribution $F(z)$ excited by a physical distributed source $S(z)$ can be synthesized in terms of the GF as follows:

$$F(z) = \iint_{\substack{\text{Source} \\ \text{region}}} dz' S(z') g(z, z', \lambda). \quad (10)$$

2.3. Relation between source-free and source-driven problems

The GF problem in the physical domain formulated in Eq. (2a) differs from the eigenvalue problem in Eq. (3) due to the presence of the (delta function) source terms on the right-hand side. A link between these two (i.e., between source-driven and source-free regimes) is established by integrating the eigenfunction expansion (Eq. (7)) along an infinite contour C_λ enclosing all of the pole singularities of g , at $\lambda = \lambda_n$, in the complex λ -plane (see Figure 2), and by invoking the residue theorem [3]:

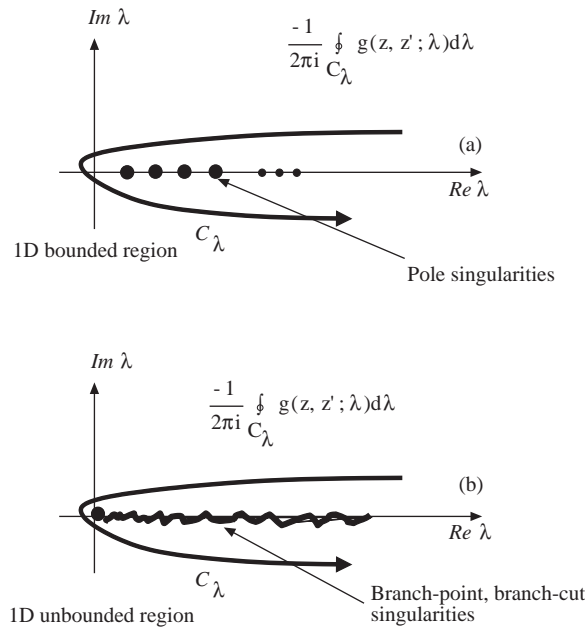


Figure 2. The singularities and the integration contour in the complex λ plane (a) bounded region with discrete eigenvalues (poles). (b) Unbounded region with continuous eigenvalues (branch cut).

$$\begin{aligned} \frac{-1}{2\pi j} \oint_{C_x} g_z(z, z'; \lambda) d\lambda &= \sum_{n=1}^{\infty} U_{zn}(z) U_{zn}(z') \left(\frac{1}{2\pi j} \oint_{C_{\lambda_n}} \frac{d\lambda}{\lambda - \lambda_n} \right) \\ &= \sum_{n=1}^{\infty} U_{zn}(z) U_{zn}(z') = \delta(z - z') \end{aligned} \tag{11}$$

In Eq. (11), C_{λ_n} (in the bracketed term) is a closed contour around each pole location $\lambda = \lambda_n$ yielding unity by the residue theorem (see Figure 2). The last equality follows from Eq. (6). This yields the desired construction of the completeness relation (delta function representation) in terms of a contour integral over the closed form spectral GF,

$$\delta(z - z') = \frac{-1}{2\pi j} \oint_{C_\lambda} g_z(z, z'; \lambda) d\lambda, \tag{12}$$

which plays a critical role in generating alternative representations for most of the field representations. The GF has the property that it decays exponentially at $|\lambda| \rightarrow \infty, Im\{\lambda\} \neq 0$ (see [1], Sec. 3.4, and see

[2], Sec.3]). Therefore, the open contour C_λ can be terminated anywhere at $\lambda \rightarrow \infty, Im\{\lambda\} \neq 0$ because the connecting path segments at $|\lambda| = \infty$ do not contribute when invoking Cauchy's theorem. When the eigenvalue spectrum is continuous (e.g., SL3 type problems), the GF has a branch point singularity and the residue series is replaced by an integration along C_λ around the spectral branch cut along the real λ -axis (see Figure 2b).

As stated above in Eq. (10), any field distribution $F(z)$ (permissible transverse profile) can be constructed via the eigenfunctions of the problem geometry by using proper modal excitation coefficients K_n

$$F(z) = \sum_n K_n U_n(z) \quad (13)$$

and the modal excitation coefficients are derived from the orthonormality property [3] as

$$K_n = \int_{z=z_1}^{z=z_2} F(z) U_n(z) dz \quad (14)$$

It should be noted that eigenfunction expansion of a given source function for SL1 and SL2 problems (i.e., finite spatial region with discrete eigenvalues) is nothing but using a Fourier series expansion of an arbitrary function in a finite region.

3. Helmholtz Equation in 2D Environments

If an SL equation is the most important equation in 1D, then the Helmholtz equation (HE) is the most important, and simplest, eigenvalue equation in 2D. Suppose a 2D guiding region comprising fixed boundaries or interfaces, an interior guiding inhomogeneous medium profile, or both, in separable (u, v) coordinates is as pictured in Figure 3. The wavenumber in the guiding region is written as $k(u, v)$. Transverse energy confinement due to the fixed boundaries "1", and by virtual boundaries (i.e., caustics [4]) "2" are pictured. For the refractively trapped modes confined by interior caustics, the mode field exterior to the caustics is evanescent (wiggly arrows), but it may become leaky with energy transfer into the exterior regions if these are accessible.

Spectral representations of fields are structured around discrete (or continuous) sums (or integrals) extending over complete (preferably orthogonal) sets of eigen (basis) functions that are matched to the problem conditions. The 2D HE problem (for the mode index n) may be postulated via

$$\{\nabla_{u,v}^2 + k^2\} W_n(u, v) = 0, \quad \nabla_{u,v}^2 = \frac{1}{h_u h_v} \left\{ \frac{\partial}{\partial u} \frac{h_v}{h_u} \frac{\partial}{\partial u} + \frac{\partial}{\partial v} \frac{h_u}{h_v} \frac{\partial}{\partial v} \right\} \quad (15)$$

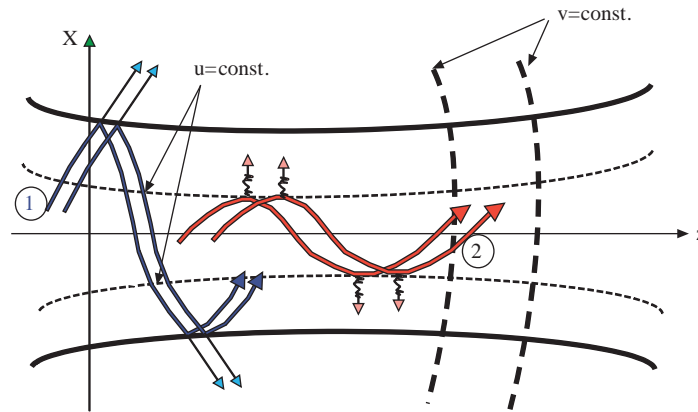


Figure 3. The 2D guiding region comprising fixed boundaries or interfaces, interior guiding inhomogeneous medium profile, or both, in separable (u, v) coordinates, and transverse energy confinement due to the fixed boundaries “1”, and by virtual boundaries (i.e., caustics [4]) “2”.

together with the trapping BCs on u -coordinate and the radiation condition when $v \rightarrow \pm\infty$. Here, h_u, h_v , are the metrics along the coordinates u and v , respectively. If it is separable in the (u, v) coordinate frame, then wave fields can be obtained by applying the separation of variables method

$$W_n(u, v) = A_n(v) U_n(u) \tag{16}$$

and the reduced 1D equations become

$$\left\{ \frac{1}{h_u h_v} \frac{\partial}{\partial v} \frac{h_u}{h_v} \frac{\partial}{\partial v} + \beta_n^2 \right\} A_n(v) = 0 + \text{radiation BCs} \tag{17}$$

$$\left\{ \frac{1}{h_u h_v} \frac{\partial}{\partial u} \frac{h_v}{h_u} \frac{\partial}{\partial u} + k_u^2 \right\} U_n(u) = 0 + \text{trapping BCs} \tag{18}$$

where $k^2 = k_u^2 + \beta_n^2$. Together with the BCs, Eq. (17) and Eq. (18) can be used to construct the exact solution. The 2D GF of Eq. (15), when the right-hand side has delta function source terms, may be constructed in a similar way described in Sec. 2.

4. A Canonic Problem: Homogeneously Filled 2D Non-Penetrable Parallel Plate Waveguide

The presentation of an SL equation and the relation between the source-free and source-driven problems is given in this section via the 2D parallel plate homogeneous waveguide with PEC boundaries (i.e., DBC for the TE_z problem, and NBC for the TM_z problem). The PEC parallel plate waveguide, with height d has its propagation direction along the z -coordinate of a Cartesian system extending from $-\infty$ to $+\infty$ along the y - and z -directions (see Figure 4). One can use Maxwell’s curl equations to end up with the GF problem associated with both the TE_z (E_y, H_x , and H_z , excited by either of M_y, J_x , or J_z) and TM_z (E_x, E_z , and H_y excited by either of M_x, M_z , or J_y) sets [2] by the equation

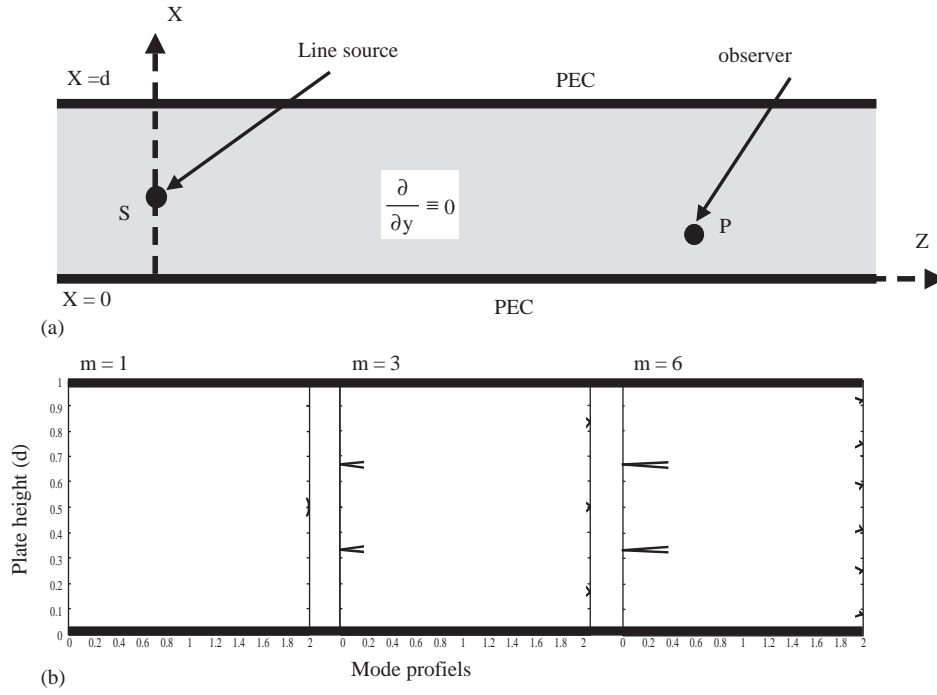


Figure 4. (a) The 2D homogeneously filled, parallel plate waveguide with perfectly conducting boundaries (d = plate height, S = source point, P = observation point). (b) Various eigenfunction profiles.

$$\left\{ \frac{\partial^2}{\partial x^2} + \frac{\partial^2}{\partial z^2} + k^2 \right\} g(x, z; x', z') = -\delta(x - x')\delta(z - z') \quad (19)$$

with BCs

$$g(x, z; x', z') = 0 \text{ at } x = 0, d \quad (TE_z) \quad (20a)$$

$$\frac{\partial}{\partial x} g(x, z; x', z') = 0 \text{ at } x = 0, d \quad (TM_z) \quad (20b)$$

$$\text{outgoing wave (radiation) condition at } z \rightarrow \pm\infty \quad (20c)$$

Here, (x', z') and (x, z) specify source and observation points, respectively. The HE problem (i.e., 2D source-free, homogeneous wave equation plus appropriate BCs) is then given as

$$\left\{ \frac{\partial^2}{\partial x^2} + \frac{\partial^2}{\partial z^2} + k^2 \right\} U(x, z) = 0 \quad (21)$$

subject to the BCs

$$U(x, z) = 0 \text{ at } x = 0, d \text{ and radiation condition, while } z \rightarrow \pm\infty. \quad (22)$$

Consider decomposition

$$U(x, z) = U_x(x)U_z(z) \quad (23)$$

where U_x satisfies the first and U_z satisfies the second BC in Eq. (22), respectively. Substituting Eq. (23) into Eq. (21), performing the partial derivatives, and rearranging the result, one finds

$$-\frac{U_x''}{U_x} = \frac{U_z''}{U_z} + k^2 \quad (24)$$

where a prime denotes the derivative with respect to the argument. Since the left-hand side in Eq. (24) is a function of x only, while the right-hand side is a function of z only, and the equation is valid for arbitrary (x, z) in the domains of Eq. (22), each side must be a constant, which is denoted by k_x^2 . Thus, Eq. (21) is reduced to 2 separate ordinary differential equations,

$$U_x'' + k_x^2 U_x = 0, \quad 0 \leq x \leq d, U_x = 0 \text{ at } x = 0, d \quad (25a)$$

$$U_z'' + k_z^2 U_z = 0, \quad -\infty < z < +\infty, \text{ radiation condition at } z \rightarrow \pm\infty \quad (25b)$$

$$k^2 = k_x^2 + k_z^2. \quad (25c)$$

The solution of the HE under DBC (TE_z) is

$$U(x, z) = E_y(x, z) = \sqrt{\frac{2}{d}} \sum_{n=1}^{\infty} \text{Sin}(k_x x) e^{-j\beta_n z} \quad (26)$$

(see Figure 4b for various mode shapes). The other 2 field components can be derived from

$$H_x(x, z) = \frac{1}{j\omega\mu_0} \frac{\partial}{\partial z} E_y(x, z) = \frac{-\beta}{\omega\mu_0} \sqrt{\frac{2}{a}} \sum_{n=1}^{\infty} \text{Sin}(k_x x) e^{-j\beta_n z} \quad (26a)$$

$$H_z(x, z) = \frac{-1}{j\omega\mu_0} \frac{\partial}{\partial x} E_y(x, z) = \frac{-k_x}{j\omega\mu_0} \sqrt{\frac{2}{a}} \sum_{n=1}^{\infty} \text{Cos}(k_x x) e^{-j\beta_n z} \quad (26b)$$

The solution of the HE under NBC (TM_z) is

$$U(x, z) = H_y(x, z) = \sqrt{\frac{2}{d}} \sum_{n=1}^{\infty} \text{Cos}(k_x x) e^{-j\beta_n z} \quad (27)$$

and, the other 2 field components are obtained as

$$E_x(x, z) = \frac{-1}{j\omega\varepsilon_0} \frac{\partial}{\partial z} H_y(x, z) = \frac{\beta}{\omega\varepsilon_0} \sqrt{\frac{2}{a}} \sum_{n=1}^{\infty} \text{Cos}(k_x x) e^{-j\beta_n z} \quad (27a)$$

$$E_z(x, z) = \frac{1}{j\omega\varepsilon_0} \frac{\partial}{\partial x} H_y(x, z) = \frac{-k_x}{j\omega\varepsilon_0} \sqrt{\frac{2}{a}} \sum_{n=1}^{\infty} \text{Sin}(k_x x) e^{-j\beta_n z} \quad (27b)$$

Both types of solutions have the same longitudinal and transverse wavenumbers

$$\beta_n = \sqrt{k_0^2 - k_x^2}, k_x = \frac{n\pi}{d}, \quad n = 1, 2, 3, \dots, \quad (28)$$

respectively. The summation (mode) index n , in both Eq. (26) and Eq. (27) starts from “1”. It should be noted that $n = 0$ in TM_z formulation is treated separately and represents TEM_z case

$$H_y(x, z) = \sqrt{\frac{2}{d}} e^{-jk_0 z} \quad (29a)$$

$$E_x(x, z) = \frac{\beta}{\omega\varepsilon_0} \sqrt{\frac{2}{d}} e^{-jk_0 z}, \quad \eta_0 = \frac{E_x(x, z)}{H_y(x, z)} = \frac{\beta}{\omega\varepsilon_0} = \sqrt{\frac{\mu_0}{\varepsilon_0}} = 377\Omega \quad (29b)$$

$$E_z(x, z) = 0 \quad (29c)$$

(with no lower frequency bound as opposed to TE_z and TM_z cases). Following either Eq. (7) or Eq. (8), the 2D GF $g(x, z; x', z')$ for the TE_z problem may be constructed as [4]

$$g(x, z; x', z') = \sum_{n=1}^{\infty} \left\{ \left(\frac{2}{d} \right) \sin\left(\frac{n\pi x}{d}\right) \sin\left(\frac{n\pi x'}{d}\right) \right\} \frac{e^{-j\beta_n |z-z'|}}{2j\beta_n} \quad (30)$$

This is convenient for evaluating the waveguide field away from the source plane $z = z'$ when the number of propagating modes with real β_n (i.e., $k_0 > n\pi/d$) is not too large. Since $\text{Im}\{\beta_n\} \leq 0$, the higher order non-propagating modes with $k_0 < n\pi/d$ decay along z . Finally, the completeness relation is

$$\delta(x - x') = \frac{2}{d} \sum_{n=1}^{\infty} \text{Sin}(k_x x) \text{Sin}(k_x x') \quad (31)$$

It is interesting to note that the eigenvalues of the problem can be extracted from the propagation characteristics as an alternative to the link between source-free and source-driven formulations, for example, as in Eq. (11). Any transverse wave function (e.g., a transmitting antenna field profile) accumulates eigen characteristics of the medium, while longitudinally propagating. Consider

$$F(x, z_0) = \sqrt{\frac{2}{d}} \sum_{n=1}^{NM} K_n \text{Sin}\left(\frac{n\pi}{d}x\right) e^{-j\beta_n z} \quad (32)$$

as the eigenfunction expansion of the initial profile at the initial range $z = z_0$, with excitation, the coefficients K_n specified from Eq. (14) (z replaced by x) and NM is the maximum number of modes that are required to represent the initial field profile “adequately”. A longitudinal correlation function may be built, while propagating this field profile through the waveguide [5,6]

$$P(z) = \int_{x=0}^{x=d} F(x, z_0) F(x, z) dx = \sum_{n=1}^{NM} K_n^2 e^{-j\beta_n z} \int_{x=0}^{x=d} \sqrt{\frac{2}{d}} \text{Sin}^2\left(\frac{n\pi}{d}x\right) dx = \sum_{n=1}^{NM} K_n^2 e^{-j\beta_n z} \quad (33)$$

Since the integral over transverse domain is equal to “1” (because of the orthonormality condition), the Fourier transformation of this correlation function yields the line spectra

$$P(\beta) = \sum_{n=1}^{NM} K_n^2 \delta(\beta - \beta_n) \quad (34)$$

i.e., the eigenvalues and excitation coefficients. However, since the data is available only in a finite range interval, a suitable windowing function better be applied to reduce aliasing effects [5]. The Fourier transform may be performed numerically via DFT (Discrete Fourier Transform) or FFT (Fast Fourier Transform); therefore, the longitudinal correlation function should be observed long enough to meet maximum longitudinal wavenumber (β_{\max}) and wavenumber resolution ($\Delta\beta$) via the relations [7] (i.e., Nyquist sampling criteria)

$$\beta_{\max} = \frac{\pi}{2\Delta z} \text{ and } \Delta\beta = \frac{2\pi}{z_{\max}} \quad (35)$$

where Δz and z_{\max} are range step size and maximum range, respectively.

5. Numerical Illustration Via Matlab Package

A simple Matlab package has been prepared for the numerical illustrations. Figure 5 and Table 2 show the flow chart and the m-file of the package, respectively. The package builds a given vertical input field profile in terms of eigenfunctions with the help of numerically computed excitation coefficients and then propagates it longitudinally. While propagating, it constructs the longitudinal correlation function as defined in Eq. (33). Finally, the FFT is applied to this correlation function and the line spectrum is obtained. The package assumes a Gaussian initial field profile

$$sgauss(x) = e^{-\left(\frac{x-hh}{tt}\right)^2} \quad (36)$$

Table 2. Matlab m-file of the package.

```

%
% Program      : PPWAVEGUIDE.m
% Author       : L. Sevgi
% Date        : June 2004
% Lecture     : EM 303 EM Waves
% Purpose     : To derive eigenvalues from longitudinal correlation function
%
=====
clear all
% ===== Get input parameters =====
d = input('Plate height (e.g., d = 1) = ');
fr = input('Frequency (e.g., fr = 8e8) = ');
hh = input('Vertical source location (e.g., hh = 0.77) = ');
tt = input('Vertical source extend (e.g., tt = 0.1) = ');
mm = input('Number of Modes (e.g., mm = 20) = ');
% ===== Calculate other parameters =====
nx = 128; delx = d/(nx-1); c = 3.E8; k0 = (2*pi*fr)/c;
% ===== Source profile =====
for k = 1:nx
    xx(k) = (k-1)*delx;    sgauss(k) = exp(-((xx(k)-hh)/tt)^2);
end
% ===== Get propagation constants (beta) =====
mp = 0;
for n = 1:mm
    if k0 > ((n*pi)/d)
        beta(n) = sqrt(k0^2-(n*pi./d)^2);
        mp = mp+1;
    else
        beta(n) = i*sqrt((n*pi./d)^2-k0^2);
    end
end
fprintf(1,'Number of propagating modes = %4.0f\n', mp);
% ===== Use orthonormality for excitation coefficients =====
for m = 1:mm
    for n = 1:nx
        ff(n) = sgauss(n)*sqrt(2./d)*sin((m*pi*xx(n))/d);
    end
    kn(m) = trapz(ff,xx);
end
% ===== Calculate Correlation Parameters =====
Betamax = 1.25*k0; dbeta = 0.05*(abs(beta(mp-1))-abs(beta(mp)));
nz0 = 2.*betamax/dbeta; k = round((log(nz0)+1))+1; nz = 2^k;
delz = pi/betamax; zmax = nz*delz; dbeta = 2.*pi/zmax;
% ===== Build initial profile =====
for k = 1:nx
    ff(k) = 0.0;
    for n = 1:mm
        ff(k) = ff(k) + kn(n)*sqrt(2./d)*sin((n*pi*xx(k))/d);
    end
end
% ===== Build longitudinal correlation function pz =====
for kk = 1:nz
    zz(kk) = (kk-1)*delz;
    xbeta(kk) = -betamax + (kk-1)*dbeta;
    for k = 1:nx

```

Table 2. Contunied.

```

    gg(k) = 0.0;
    for n = 1:mp
        gg(k) = gg(k) + kn(n)*sqrt(2./d)*sin(n*pi*xx(k)/d)*exp(i*beta(n)*zz(kk));
    end
    end
    p = ff.*gg;
    corel(kk) = trapz(xx,p);
    end
% ===== apply Hanning window =====
for kk = 1:nz
    corel(kk) = 0.5*(1.-cos(2.*pi*zz(kk)/zmax))*corel(kk);
end
% ===== Take fft of correlation function =====
corel2 = fftshift(corel); corelf = fft(corel,nz); corelf0 = fftshift(corelf);
% ===== Plot output =====
figure (1);           % Initial field profiles
colordef black;
plot(sgauss, xx, abs(ff),xx,'r--','LineWidth',2,'MarkerSize',5)
figure (2);           % final field profile
plot(xx, abs(gg), 'LineWidth',2)
figure (3);           % Correlation function vs. range
plot(zz, corel, 'LineWidth',2)
figure (4);           % Line spectra vs. eigenvalue
bmax = betamax + betamax/5.;
plot(xbeta, abs(corelf0), 'LineWidth',2)
xlim([0,bmax]);

```

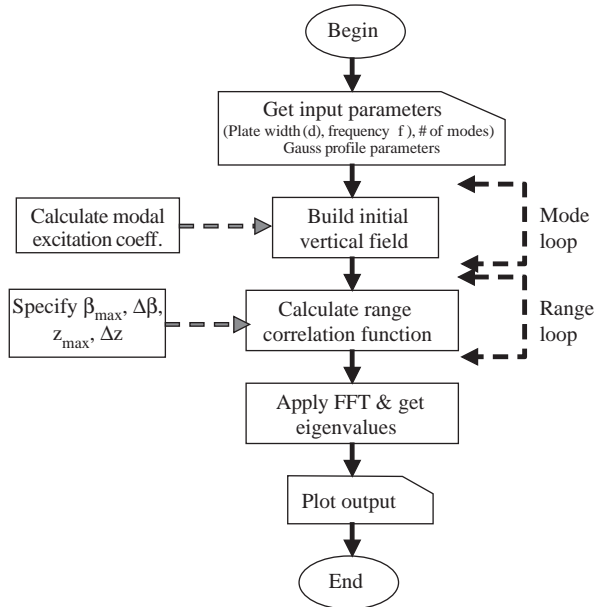


Figure 5. The flow chart of the Matlab package.

where hh and tt are vertical source position and vertical source extend, respectively. The user supplies initial parameters; width of the parallel plate (d), operating frequency (fr), vertical source position hh , vertical source extend tt , and the number of modes mm . The number of vertical points (nx) is chosen as 128 in the

package. Once the user-supplied parameters are in, the package computes the vertical step ($delx$) and the wavenumber (k_0). The 1D arrays $xx(nx)$, $sgauss(nx)$, and $beta(mm)$ are reserved for the vertical points; initial Gauss field values at these points and mm eigenvalues for both propagating and non-propagating modes. The number of propagating modes (mp) (with real eigenvalues) is displayed by the package. Then, excitation coefficients ($kn(mm)$) are calculated by using the orthonormality property of the eigenfunctions, and the initial field profile is reproduced (and stored in the array $ff(nx)$) in terms of mm eigenfunctions. The first plot in the package gives initial height profiles $sgauss$ and ff vs. xx . The user may change mm and observe graphically whether or not the number of given modes is adequate to represent the given Gaussian field profile. An example is given in Figure 6 for the parameters $d = 1m$, $fr = 800 MHz$, $h = 0.77m$. Three different tt values are used for the source extend; $tt = 0.1$, $tt = 0.05$, and $tt = 0.01$. It is tested that addition of the first 15 and 25 modes adequately represent the Gaussian field profile (see the first 2 plots in Figure 6), but more than one hundred modes are required when $tt = 0.01$ (see the last plot in Figure 6).

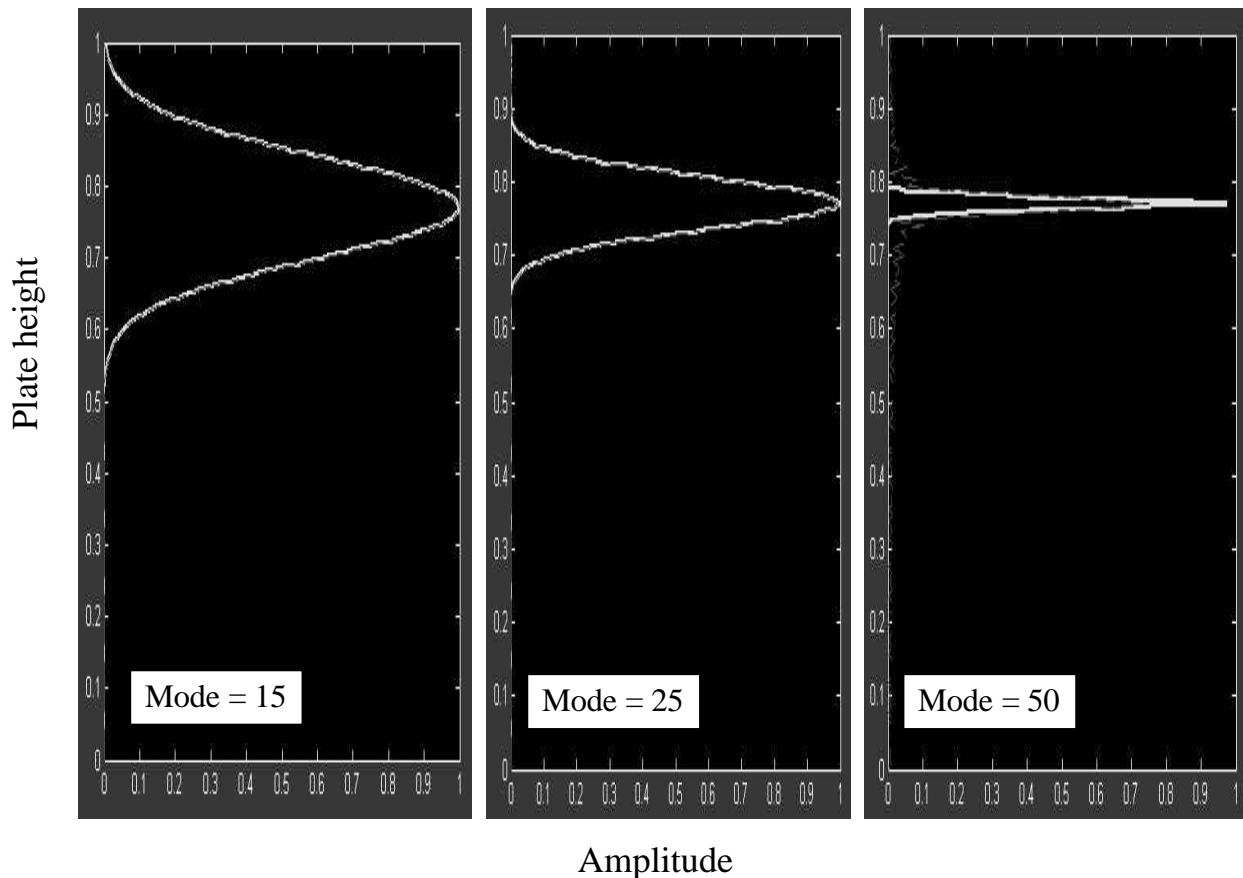


Figure 6. Field profile vs. plate height (the parameters are $d = 1m$, $fr = 800MHz$, $h = 0.77m$, $tt = 0.1$ (left), $tt = 0.05$ (middle), $tt = 0.01$ (right)).

Figure 7 plots vertical field distributions at different ranges, where solid and dashed curves correspond to the solutions with all given modes (i.e., propagating and non-propagating) and only propagating modes, respectively. Indistinguishable agreement shows that only propagating modes contribute wavefields inside the waveguide away from the source.

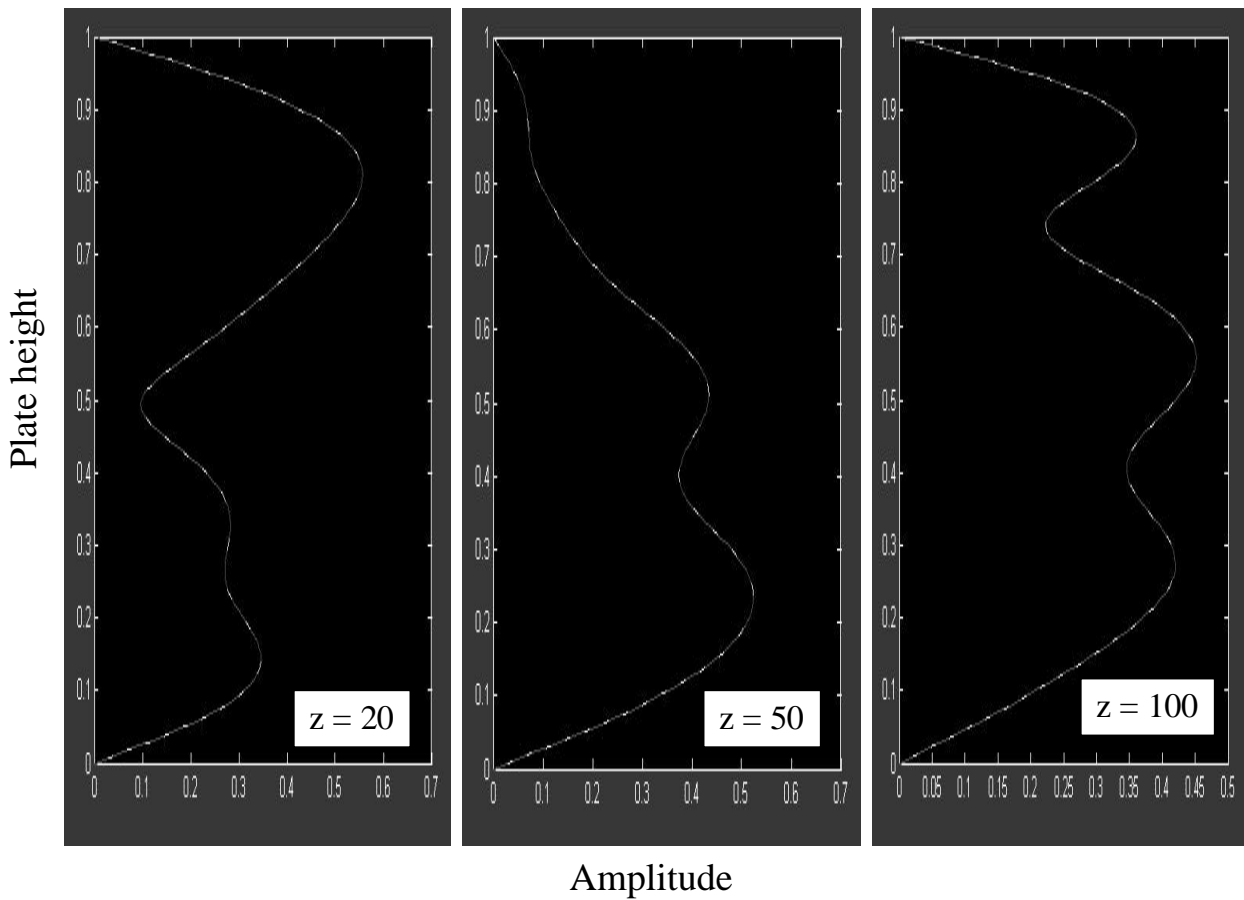


Figure 7. Field profile vs. plate height at ranges $z = 20m$, $z = 50m$, $z = 100m$ (the parameters are $d = 1m$, $rfr = 800MHz$, $h = 0.77m$, $tt = 0.1$).

The longitudinal correlation function $corel(nz)$ is then calculated by using Eq. (35), after the specification of the required parameters. Maximum longitudinal wavenumber β_{max} is chosen to be slightly greater than free space wavenumber k_0 . The resolution $\delta\beta$ is taken as $1/5$ of the shortest distance between the eigenvalues (i.e., $\beta(2) - \beta(1)$). The number of range steps nz is specified according to Eq. (35). In order to do that, nz is rounded up to the next integer that is a multiple of 2 (which is required for further FFT analyses). The output is smoothed by using a Hanning window and finally its FFT is taken and stored in $corelf0(nz)$. The second, third and fourth plots in the package belong to field vs. height at the last range, correlation function vs. range, and FFT of the correlation function vs. longitudinal wavenumber, respectively. Figure 8 presents (a) the correlation function and (b) its line spectra for the same set of parameters used in Figure 6. Only the first 5 modes have real longitudinal eigenvalues (therefore, can propagate inside the waveguide) and their contribution can easily be distinguished in the figure. It should be noted that the resolution in the eigenvalue domain can be improved (i.e., $\Delta\beta$ decreased) and better line spectra can be obtained, as shown in Figure 9.

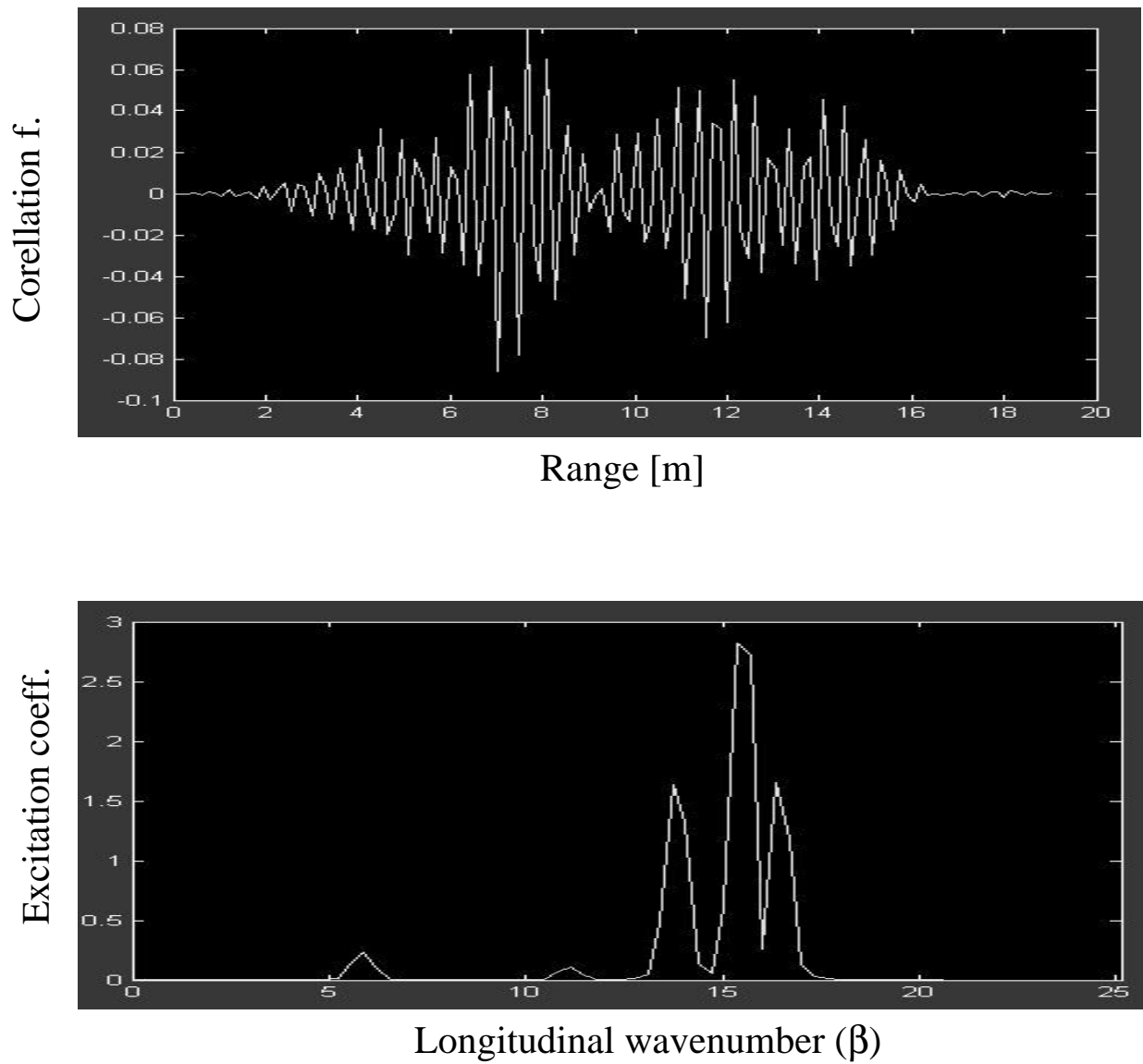


Figure 8. (a) Correlation function vs. range ($0 < z < 20$) (the parameters $d = 1m$, $fr = 800MHz$, $h = 0.77m$, $tt = 0.1$). (b) Line spectra (eigenvalues) in longitudinal wavenumber domain (only the first 5 modes are propagating and they are distinguished in the plot; eigenvalues and excitation coefficients are: $\beta_1 = 16.7552$, $a_1 = -0.0986$, $\beta_2 = 15.5324$, $a_2 = 0.1440$, $\beta_3 = 13.8531$, $a_3 = -0.1148$, $\beta_4 = 11.0825$, $a_4 = 0.0324$, $\beta_5 = 5.8305$, $a_5 = 0.0547$).

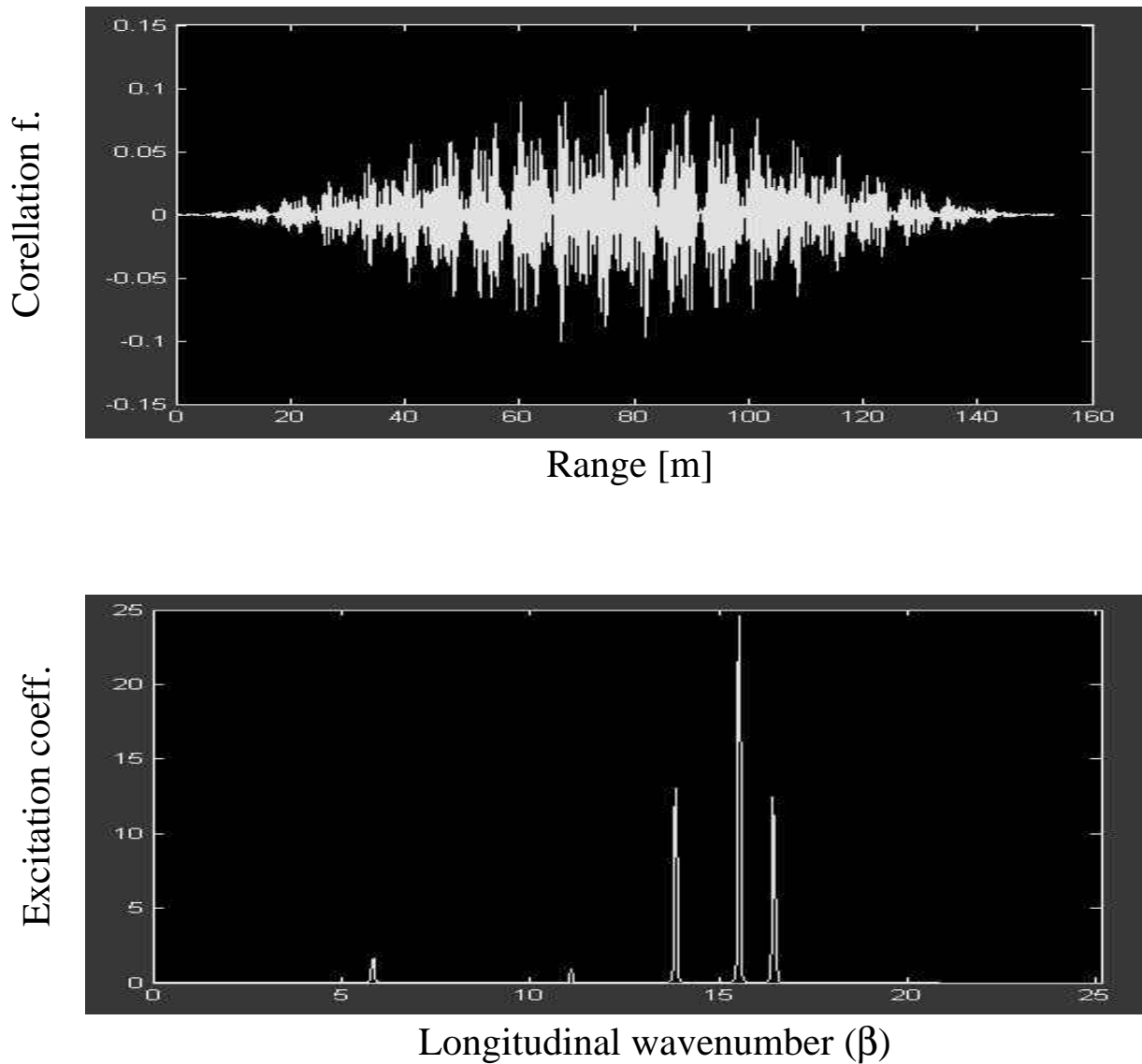


Figure 9. (a) Correlation function vs. range ($0 < z < 160$) (the parameters $d = 1m$, $fr = 800MHz$, $h = 0.77m$, $tt = 0.1$). (b) Line spectra (eigenvalues) in longitudinal wavenumber domain (eigenvalues and excitation coefficients are same as Figure 8).

6. Conclusions and Discussions

The Sturm-Liouville (SL) equation has been taken into account in this tutorial article. Source-free (eigenvalue) and source-driven (GF) formulations derived from the SL equation have been discussed. Emphasis has been placed on a canonical structure, the 2D PEC parallel plate waveguide, and propagation inside this waveguide has been investigated, both as eigenvalue and GF problems. A Matlab package has been prepared and used in numerical illustrations.

Canonical problems mostly belong to non-physical structures or idealized geometries, but they serve as a reference for calibration, verification, etc., and are the best to give physical insight. It is extremely difficult, and sometimes impossible, to analytically solve realistic engineering problems. Fortunately, there

are powerful numerical simulators that can be applied to most of 2D (even 3D) waveguiding structures. The split step parabolic equation (SSPE) in use for many decades ([8] is a comprehensive source for SSPE-related studies and references and is very effective in modeling frequency-domain (FD) one-way propagation problems. Time-domain propagators [9-11] based on the finite-difference of time-domain (FDTD) and transmission line matrix (TLM) techniques have also been introduced, and are very promising for numerical broadband pulse propagation modeling. The strategy presented here, therefore, can be extended to many propagation problems whose analytical solutions are not available, yet the eigenfunctions and eigenvalues can numerically be computed by using these FD and TD numerical propagators.

References

- [1] L. B. Felsen and N. Marcuvitz, *Radiation and Scattering of Waves*, Prentice-Hall, Englewood Cliffs, New Jersey, 1973, Classic reissue IEEE Press, 1994.
- [2] D. G. Dudley, *Mathematical Foundations for Electromagnetic Theory*, IEEE Press (Series on Electromagnetic Waves), New York, 1994.
- [3] R. E. Collin, *Field Theory of Guided Waves*, McGraw-Hill, Inc., New York, 1960.
- [4] L. B. Felsen, F. Akleman and L. Sevgi, "Wave Propagation Inside a Two-dimensional Perfectly Conducting Parallel Plate Waveguide: Hybrid Ray-Mode Techniques and Their Visualizations", *IEEE Antennas and Propagation Magazine*, vol. 46, no. 6, pp. 69-89, Dec 2004.
- [5] M. D. Feit and Jr. J. A. Fleck, "Computation of Mode Properties in Optical Fiber Waveguides by a Beam Propagating Method", *Applied Optics*, vol. 19, no. 7, pp. 1154-1164, 1980.
- [6] L. Sevgi and E. Topuz, "Split step Parabolic Equation analysis of Coupled Dielectric Waveguides", *ELEKTRİK, Turkish J. of Electrical Engineering and Computer Sciences*, vol. 3, No 2-3, pp. 85-92, 1995.
- [7] L. Sevgi, *Complex Electromagnetic Problems and Numerical Simulation Approaches*, IEEE & John Wiley Press, NY, June 2003.
- [8] M. Levy, *Parabolic equation methods for electromagnetic wave propagation*, IEE, Institution of Electrical Engineers, 2000.
- [9] F. Akleman and L. Sevgi, "A Novel Time-domain Wave Propagator", *IEEE Trans. on Antennas and Propagat*, vol. 48, no. 5, pp. 839-841, 2000.
- [10] M. O. Özyalçın, F. Akleman and L. Sevgi, "A Novel TLM Based Time Domain Wave Propagator", *IEEE Trans. on Antennas and Propagat.*, vol. 51, no. 7, pp. 1679-1683, 2003.
- [11] L. Sevgi, F. Akleman and L. B. Felsen, "Ground Wave Propagation Modeling: Problem-matched Analytical Formulations and Direct Numerical Techniques", *IEEE Antennas and Propagation Magazine*, vol. 44, no. 1, pp. 55-75, 2002.